Maximal Overlap and Sensitivity
of a VIRGO Pair to Graviton Backgrounds

D. Babusci [a] and M. Giovannini [b]

[a] *INFN- Laboratori Nazionali di Frascati, 1-00044 Frascati, Italy*
[b] *Institute for Theoretical Physics, Lausanne University,*
BSP-Dorigny, CH-1015, Switzerland

Abstract

The sensitivity of a pair of VIRGO interferometers to gravitational waves backgrounds of cosmological origin is analyzed for the cases of maximal and minimal overlap of the two detectors. The improvements in the detectability prospects of scale-invariant and non-scale-invariant logarithmic energy spectra of relic gravitons are discussed.

1   Introduction and motivations

Stochastic gravitational waves backgrounds [1] constitute a promising source for wideband interferometers whose operating window can be approximately located between few Hz and 10 kHz. There are no compelling theoretical reasons why in such a frequency interval we should expect a negligible energy density stored in a stochastic background of primordial origin. Listening to phenomenology, we know that, unless Ω_{GW} (the logarithmic energy spectrum of relic gravitons) is either flat or decreasing (as predicted, for instance, by some classes of inflationary models), the present constraints on stochastic gravitational waves backgrounds are quite mild. Listening to the theory we know that if Ω_{GW} increases for frequencies larger than few mHz [2], then it is indeed possible to achieve a large signal in the operating window of interferometric detectors without conflicting neither with the fractional timing error of the millisecond pulsar's pulses [3] nor with the requirement that the total energy density of relic gravitons should be smaller than the total amount of relativistic matter at nucleosynthesis [4]. These qualitative features can easily emerge in different models based on diverse physical frameworks including quintessential inflationary models [5], dimensional decoupling [6], early violations of the dominant energy conditions [7] and superstring theories [8, 9].

Recently the proposal of building in Europe an advanced interferometer of dimensions comparable with VIRGO [10] has been carefully scrutinized [11]. In view of this idea we would like to determine what would be the sensitivity of the correlation between two VIRGO-like detectors to a generic stochastic graviton background. The answer to this question depends upon two experimental informations (i.e. the specific form of the noise power spectra and the relative location and orientation of the two detectors) and upon the theoretical form of the logarithmic energy spectrum. Concerning the last point, the specific frequency dependence of $\Omega_{\mathrm{GW}}(f)$ is extremely relevant. In fact $\Omega_{\mathrm{GW}}(f)$ directly enters in the expression of the signal-to-noise ratio (SNR) [12, 13] and, therefore, logarithmic energy spectra with a different frequency dependence will lead, necessarily, to different SNR [14]. Given a theoretical model, in order to compute reliably the sensitivity we have to specify the location of the two VIRGO detectors and the form of the noise power spectra. Thus, it is important to analyze how the relative distance between the two detectors of the pair can affect the sensitivity to the specific logarithmic energy spectrum of relic gravitons we ought to detect. In this respect, scale-invariant and non-scale-invariant logarithmic energy spectra lead to different sensitivity levels for the VIRGO pair already under the assumption that no improvement in the reduction of the thermal noises will take place prior to the construction of the second VIRGO detector. If a reduction in the contribution of the pendulum and pendulum's internal modes to the noise power spectra is achieved the improvements in the sensitivity will be even sharper [15].

2   Maximal and minimal overlap

In the hypothesis that the graviton background is isotropic and unpolarized the reduction of the sensitivity due to the relative distance and orientation of the two detectors depends upon the frequency f and it is usually parameterized in terms of the (dimensionless) overlap reduction function [13].

By denoting (in spherical coordinates) with $\hat{\Omega} = (\cos\phi\sin\theta, \sin\phi\sin\theta, \cos\theta)$ a generic direction along which the given gravitational wave (GW) propagates, the overlap reduction function $\gamma(f)$ can be expressed, in terms of the pattern functions F_i^A determining the response of the i-th detector ($i = 1, 2$) to the $A = +, \times$ polarizations[1]:

$$F^A(\hat{r}, \hat{\Omega}, \psi) = \mathrm{Tr}\left\{D(\hat{r})\,\varepsilon^A(\hat{\Omega}, \psi)\right\} \tag{1}$$

$$\gamma(f) = \frac{1}{F}\sum_A \langle e^{i2\pi f d\hat{\Omega}\cdot\hat{s}}\, F_1^A(\hat{r}_1, \hat{\Omega}, \psi)F_2^A(\hat{r}_2, \hat{\Omega}, \psi)\rangle_{\hat{\Omega},\psi} = \frac{\Gamma(f)}{F}. \tag{2}$$

Notice that $\Delta\vec{r} = \vec{r}_1 - \vec{r}_2 = d\,\hat{s}$ is the separation vector between the two detector sites and the summation over the index A has to be taken over the physical polarizations (characterized by the polarization angle ψ)

$$\begin{aligned}
\varepsilon^+(\hat{\Omega}, \psi) &= e^+(\hat{\Omega})\cos 2\psi - e^\times(\hat{\Omega})\sin 2\psi\,,\\
\varepsilon^\times(\hat{\Omega}, \psi) &= e^+(\hat{\Omega})\sin 2\psi + e^\times(\hat{\Omega})\cos 2\psi\,,
\end{aligned} \tag{3}$$

of the incoming wave. The symmetric, trace-less tensor $D(\hat{r})$ appearing in Eq. (1) depends on the geometry of the detector located in $\vec{r}$. A general analytical expression for the function $\gamma(f)$ can be written as [13]

$$\gamma(f) = \rho_0(\delta)\, D_1^{ij}\, D_{2\,ij} + \rho_1(\delta)\, D_1^{ij}\, D_{2\,i}^k\, s_j\, s_k + \rho_2(\delta)\, D_1^{ij}\, D_2^{kl}\, s_i\, s_j\, s_k\, s_l, \tag{4}$$

where

$$\begin{bmatrix} \rho_0(\delta) \\ \rho_1(\delta) \\ \rho_2(\delta) \end{bmatrix} = \frac{1}{F\delta^2}\begin{bmatrix} 2\delta^2 & -4\delta & 2 \\ -4\delta^2 & 16\delta & -20 \\ \delta^2 & -10\delta & 35 \end{bmatrix}\begin{bmatrix} j_0(\delta) \\ j_1(\delta) \\ j_2(\delta) \end{bmatrix}, \tag{5}$$

with $j_k(\delta)$ the standard spherical Bessel functions:

$$j_0(\delta) = \frac{\sin\delta}{\delta}\,, \qquad j_1(\delta) = \frac{j_0(\delta) - \cos\delta}{\delta}\,, \qquad j_2(\delta) = 3\,\frac{j_1(\delta)}{\delta} - j_0(\delta)\,,$$

where $\delta = 2\pi f d$.

---

[1] We introduced the notation

$$\langle...\rangle_{\hat{\Omega},\psi} = \int_{S^2}\frac{d\hat{\Omega}}{4\pi}\int_0^{2\pi}\frac{d\psi}{2\pi}\,(...)$$

to denote the average over the propagation direction (θ, ϕ) and the polarization angle ψ of the GW.

The normalization F is given by

$$F = \sum_A \langle F_1^A(\hat{r}_1, \hat{\Omega}, \psi) F_2^A(\hat{r}_2, \hat{\Omega}, \psi) \rangle_{\hat{\Omega}, \psi} \mid_{1 \equiv 2}, \qquad (6)$$

where the notation $1 \equiv 2$ is a compact way to indicate that the detectors are coincident and coaligned and, if at least one of the two is an interferometer, the angle between its arms is equal to $\pi/2$ (L-shaped geometry). In this situation, by definition, $\gamma(f) = 1$. When the detectors are shifted apart (so there is a phase shift between the signals in the two detectors), or rotated out of coalignment (so the detectors have different sensitivity to the same polarization) it turns out that $|\gamma(f)| < 1$. The normalization factor F is $2/5$ in the case of the VIRGO pair and in the case of any pair of wide band interferometers.

By varying the frequency f the overlap reduction function is of order one until it reaches its first zero and, then, it starts oscillating around zero. The position of this first zero is roughly proportional to the inverse of the distance d between the two detectors. The location of the corner station of the first interferometer will be assumed in Cascina (43.6 N , 10.5 E) where the VIRGO interferometer is presently under construction. The position of the second corner station is, at present, still under study. In our investigation we will suppose that the second corner station in different european sites.

On a purely theoretical ground one ought to have a situation where the overlap reduction function is as close as possible to one for most of the frequencies in the operating window of the VIRGO pair. In other words we would like to push the first zero in the ultra-violet because this would imply that the region of maximal overlap (i.e. $\gamma(f) \sim 1$) gets larger. Since an increase in the region of maximal overlap produces a decrease in the relative distance of the two interferometers it will not be possible to decrease the distance *ad libitum*. In fact, when we decrease the distance between the detectors, we might introduce correlations between the local seismic and electromagnetic noises. We will assume that a distance of approximately 50 km is sufficient to decorrelate these noises. At the moment we do not have indications against such an assumption.

The maximization of the overlap constitutes an important component as we can argue from the full expression of the signal-to-noise ratio. For the correlation of two interferometers, under the assumptions that the detector noises are Gaussian, much larger in amplitude than the gravitational strain and statistically independent on the strain itself, it can be shown [12, 13] that the signal-to-noise ratio in a frequency range $(f_\mathrm{m}, f_\mathrm{M})$ is given, for an observation time T, by [2]

$$\mathrm{SNR}^2 = \frac{3H_0^2}{5\sqrt{2}\,\pi^2} \sqrt{T} \left\{ \int_{f_\mathrm{m}}^{f_\mathrm{M}} \mathrm{d}f \, \frac{\gamma^2(f)\, \Omega_{\mathrm{GW}}^2(f)}{f^6\, S_n^{(1)}(f)\, S_n^{(2)}(f)} \right\}^{1/2}, \qquad (7)$$

where H_0 is the present value of the Hubble parameter. In Eq. (7), the performances achievable by the pair of detectors is controlled by the noise power spectra (NPS) $S_n^{(1,2)}$, whereas $\Omega_{\mathrm{GW}}(f)$ is the *theoretical* background signal defined through the logarithmic energy

---

[2] We follow the notations of Refs.[14, 15]

spectrum, normalized to the critical density ρ_c, and expressed at the present (conformal) time[3] η_0

$$\Omega_{\mathrm{GW}}(f, \eta_0) = \frac{1}{\rho_c} \frac{\mathrm{d}\rho_{\mathrm{GW}}}{\mathrm{d}\ln f} = \overline{\Omega}(\eta_0)\,\omega(f, \eta_0)\,. \tag{8}$$

It is intuitively clear, from the combined analysis of the two previous expressions, that if $\gamma(f)$ reaches its first zero a low frequencies, the value of the integral will be smaller than in the case where $\gamma(f)$ reaches its first zero at larger frequencies.

3 Overlap versus noise power spectra

Given a specific logarithmic energy spectrum of primordial gravitons the signal-to-noise ratio is determined by the interplay between the overlap reduction function and the noise power spectra of the detectors. The noise power spectrum of the VIRGO detector can be approximated by an analytical fit [16], namely

$$\Sigma_n(f) = \frac{S_n(f)}{S_0} = \begin{cases} \infty & f < f_b \\ \Sigma_1\left(\dfrac{f_a}{f}\right)^5 + \Sigma_2\left(\dfrac{f_a}{f}\right) + \Sigma_3\left[1 + \left(\dfrac{f}{f_a}\right)^2\right], & f \geq f_b \end{cases} \tag{9}$$

where

$$S_0 = 10^{-44}\,\mathrm{s}\,, \qquad f_a = 500\,\mathrm{Hz}\,, \qquad f_b = 2\,\mathrm{Hz}\,, \qquad \begin{aligned} \Sigma_1 &= 3.46 \times 10^{-6} \\ \Sigma_2 &= 6.60 \times 10^{-2} \\ \Sigma_3 &= 3.24 \times 10^{-2}\,. \end{aligned}$$

The noise power spectrum of the VIRGO detectors is reported in Fig. 1. In our parametrization, Σ_1 and Σ_2 control the contribution of the pendulum and pendulum's internal modes [17] to the thermal noise. Σ_3 controls instead the shot noise. For frequencies smaller than f_b the noise power spectrum goes to infinity. The different values of $\Sigma_{1,2,3}$ together with f_a and f_b define a specific noise configuration of the detectors. If, in the future, one of the contributions to the noises will be reduced, the noise power spectra will change accordingly and the noise configuration might be different. Without entering into the details of the actual experimental method which could allow such a reduction we can parametrize possible changes in the noise power spectra through a noise "reduction vector"

$$\vec{\rho} = (\rho_1, \rho_2, \rho_3) \tag{10}$$

where $\rho_i < 1$ defines the reduction in the corresponding coefficient Σ_i entering Eq. (9). Within the present noise configuration $\vec{\rho} = (1, 1, 1)$.

---

[3]In most of our equations we drop the dependence of spectral quantities upon the present time since all the quantities introduced in this paper are evaluated today.
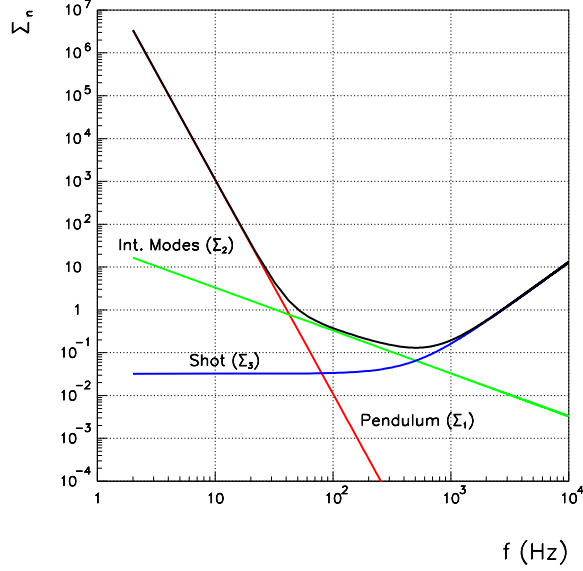
Figure 1: We report the analytical fit of the rescaled noise power spectrum Σ_n defined in Eq. (9) in the case of the VIRGO detector. With the full (thick) line we denote the total NPS. We also illustrate the separated contribution of the (gaussian and stationary) sources of noise, namely the thermal (pendulum and pendulum's internal modes) and the shot noise.

By using into Eq. (7) the expression of the theoretical spectrum given in Eq. (8) we have that the minimum normalization $\overline{\Omega}$ of a spectrum with functional variation $\omega(f)$, detectable by the VIRGO pair in an observation time T with a given SNR is determined by

$$h_0^2 \overline{\Omega} \simeq \frac{4.0 \times 10^{-7}}{J} \left(\frac{1 \text{ yr}}{T} \right)^{1/2} \text{SNR}^2 \ . \tag{11}$$

In this equation the information of the specific $\omega(f)$ is encoded in the quantity J:

$$J = \left\{ \int_{\nu_\text{m}}^{\nu_\text{M}} \text{d}\nu \, \frac{\gamma^2 \left(f_0 \nu \right) \omega^2 (f_0 \nu)}{\nu^6 \, \Sigma_n^{(1)}(f_0 \nu) \, \Sigma_n^{(2)}(f_0 \nu)} \right\}^{\frac{1}{2}} \tag{12}$$

where the integration variable is $\nu = f/f_0$ (f_0 is a generic frequency scale within the region $f_\text{m} \leq f \leq f_\text{M}$). We can assume $f_\text{M} = 10$ kHz, whereas the lower extreme f_m is put equal to the frequency f_b entering Eq. (9). The choice of f_0 is purely conventional and in view of our discussion we took $f_0 = 100$ Hz.

Following the terminology of Sec. II the curve denoted by A in Fig. 2 corresponds to the maximal overlap. The minimal overlap is represented by the curve C where the location of the second VIRGO detector coincides with the present location of the GEO [18] detector. For completeness we also illustrate a possible intermediate overlap (profile B) corresponding the situation where the two detectors are roughly 500 km far apart. In principle, the effect of
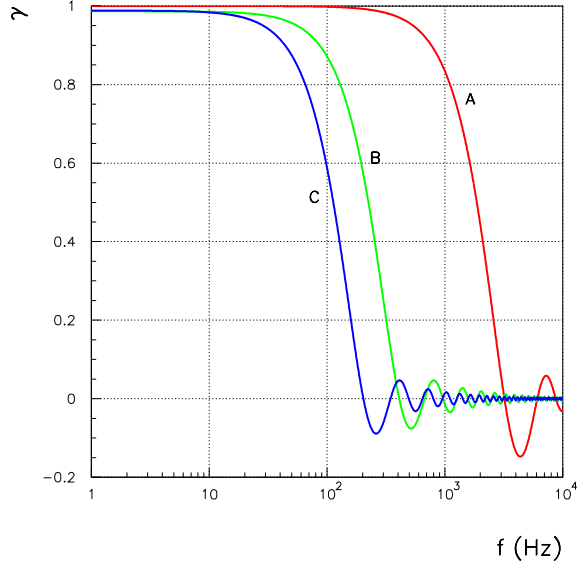
Figure 2: We report the overlap reduction function(s) for the correlation of the VIRGO detector presently under construction in Cascina (43.6 N, 10.5 E) with a coaligned interferometer whose (corner) station is located at: A) (43.2 N, 10.9 E), $d = 58$ km (Italy); B) (43.6 N, 4.5 E), $d = 482.7$ km (France); C) (52.3 N, 9.8 E), $d = 958.2$ km (Germany). The third site (C) corresponds to the present location of the GEO detector.

a maximization (or reduction) of the overlap between the two detectors of the VIRGO pair is not independent on the analytical form of the logarithmic energy spectrum $\omega(f)$. Indeed, as we will show in the following Sections a reduction in the overlap has a mild effect if the logarithmic energy spectrum is scale-invariant. However, if the logarithmic energy spectrum is non-scale-invariant (and it increases with frequency) then the effect can be sizable.

4   Scale-Invariant Energy Spectra

Suppose, as a warm-up, that $\omega(f) = 1$ so that the logarithmic energy spectrum is strictly scale-invariant. Then according to Eq. (11) the sensitivity of the VIRGO pair can be computed. Let us firstly assume that the two detectors have minimal overlap (i.e curve C in Fig. 2) and let us suppose that the VIRGO detectors will have the NPS given specifically by Eq. (9). In other words the reduction vector will have its present value $\vec{\rho} = (1, 1, 1)$. In this case, from Eq. (12) we can determine the sensitivity of the VIRGO pair. By using now into Eq. (11) the expression of the theoretical spectrum given in Eq. (8) we can determine the sensitivity of the VIRGO pair after one year of observation (i.e. $T = \pi \times 10^7$ s) and with

SNR $= 1$:

$$h_0^2 \overline{\Omega} \simeq 8.5 \times 10^{-8} \, . \tag{13}$$

Suppose now to repeat the same estimate by assuming the maximal overlap. We want also to assume that the pendulum and pendulum's internal modes are suppressed by a factor of a hundred corresponding to a noise reduction vector $\vec{\rho} = (0.01, 0.01, 1)$. Under this second set of assumptions we have that for $T = 1$ yr and SNR $= 1$ the sensitivity of the VIRGO pair becomes

$$h_0^2 \overline{\Omega} \simeq 1.9 \times 10^{-9} \, , \tag{14}$$

The two previous examples are quite extreme but a more complete analysis of the interplay between maximization of the overlap and noise reduction is illustrated in Tab. 1. In the first

Table 1: The minimum detectable $\overline{\Omega}$ for the three different location of the second VIRGO detector (see Fig. 2) as a function of the reduction noise vector $\vec{\rho}$.

$\vec{\rho}$	A	B	C
$(1, 1, 1)$	7.2×10^{-8}	7.6×10^{-8}	8.5×10^{-8}
$(1, 1, 0.1)$	6.9×10^{-8}	7.4×10^{-8}	8.3×10^{-8}
$(0.1, 1, 1)$	3.0×10^{-8}	3.1×10^{-8}	3.2×10^{-8}
$(1, 0.1, 1)$	2.5×10^{-8}	2.7×10^{-8}	3.4×10^{-8}
$(1, 0.01, 1)$	1.8×10^{-8}	2.0×10^{-8}	2.5×10^{-8}
$(0.01, 1, 1)$	1.2×10^{-8}	1.3×10^{-8}	1.3×10^{-8}
$(0.1, 0.1, 1)$	9.1×10^{-9}	9.6×10^{-9}	1.0×10^{-8}
$(0.1, 0.01, 1)$	5.7×10^{-9}	6.0×10^{-9}	6.7×10^{-9}
$(0.01, 0.1, 1)$	3.5×10^{-9}	3.6×10^{-9}	3.7×10^{-9}
$(0.01, 0.01, 1)$	1.9×10^{-9}	1.9×10^{-9}	2.0×10^{-9}

column of Tab. 1 we report the different values taken by the reduction vector $\vec{\rho}$ whereas in the second, third and fourth columns (from the left) we indicate the sensitivities achieved by a VIRGO pair under the assumption that the second (coaligned) VIRGO interferometer is located, respectively, in the three positions specified by the three profiles A, B and C of Fig. 2. The first corner station is always assumed, in our estimates, to be in Cascina.

In spite of the fact that the example of an *exactly* flat spectrum is academic and oversimplified [4] we can draw, from our exercise, few interesting hints. We can see that if no noise reduction and minimal overlap are simultaneously assumed the sensitivity is, comparatively, smaller than in the case where a selective reduction of the thermal noises and maximal overlap are postulated. If the reduction does not occur in the thermal components of the noise the improvement in the sensitivity is negligible, but still present.

Our considerations were deduced only assuming a reduction in the thermal components of the noise. In principle, we should also consider the possible effect of a reduction in the shot noise. If the reduction is selectively applied to the shot noise, the improvement in the sensitivity is negligible [15]. This can be easily understood from the analysis of Fig. 1: the shot noise starts being the dominant contribution to the NPS for $f \sim 1$ kHz, i.e. in a frequency region where the overlap begins to deteriorate (see Fig. 2). As far as the achievable sensitivity levels are concerned, we can notice that the three location are practically indistinguishable. This statement is even more accurate if the reduction in the thermal noise components gets larger.

5   Non-scale-invariant spectra

It is interesting to repeat a similar analysis in the case where $\omega(f)$, instead of being scale-invariant, increases with f. In principle we would expect that in the latter case the impact of the maximization of the overlap will be more pronounced. The reason is that the contribution of $\omega(f)$ to the integrand of Eq. (7) (or of Eq. (12)) increases at high frequencies if $\omega(f)$ increases. Therefore, if the first zero of $\gamma(f)$ falls just after 100 Hz (or possibly even before) the contribution of $\omega(f)$ will be erased more efficiently.

In order to show this behaviour let us analyze some specific examples among the ones mentioned in the introduction. For instance, in string cosmological models, the minimal pre-big-bang spectra have a two-branch form which can be expressed as [8, 9, 15]

$$
\omega(f) = \begin{cases} z_s^{-2\beta} \left(\dfrac{f}{f_s} \right)^3 \left[1 + z_s^{2\beta-3} - \dfrac{1}{2} \ln \dfrac{f}{f_s} \right]^2 & f \leq f_s = \dfrac{f_1}{z_s} \\[2em] \left[\left(\dfrac{f}{f_1} \right)^{3-\beta} + \left(\dfrac{f}{f_1} \right)^{\beta} \right]^2 & f_s < f \leq f_1 \end{cases}
\tag{15}
$$

where

$$
\beta = \frac{\ln\left(g_1/g_s\right)}{\ln z_s} \;,
\tag{16}
$$

In this formula $z_s = f_1/f_s$ and g_s are, respectively, the red-shift during, and the value of the coupling constant at the beginning of, the string phase [8, 9, 15]. The maximal amplified

---

[4]Needless to say that the analysis of the Sachs-Wolfe contribution to the detected amount of anisotropy implies, on a theoretical ground that, for $f_m < f < f_M$, $h_0^2 \Omega_{GW} \leq 10^{-15}$ if a scale-invariant spectrum was originated during inflation.

frequency f_1 of the graviton spectrum is

$$f_1(\eta_0) \simeq 64.8 \sqrt{g_1} \left(\frac{10^3}{n_r} \right)^{1/12} \text{GHz} , \qquad (17)$$

where n_r is the effective number of spin degrees of freedom in thermal equilibrium at the end of the stringy phase, and $g_1 = M_s/M_{\text{Pl}}$ is the mismatch between the string (M_s) and Planck (M_{Pl}) masses. The value of g_1 corresponds to the dilaton coupling at the beginning of the radiation dominated epoch and it can be estimated to lie between 0.3 and 0.03 [19].

In the case of increasing logarithmic energy spectra the evaluation of the sensitivity is a bit different from the case of purely flat spectra. If $\omega(f)$ grows in frequency the integrated spectrum can become, in principle large. We know, however, that the total amount of gravitons present at big-bang nucleosynthesis (BBN) cannot exceed the total amount of relativistic matter [4]. Otherwise the expansion rate of the Universe would increase too much and the observed light elements abundances could not be correctly reproduced. This implies that

$$h_0^2 \int_{f_{\text{ns}}}^{f_{\text{max}}} \Omega_{\text{GW}}(f, \eta_0) \, \text{d} \ln f \ < \ 0.2 \, h_0^2 \Omega_\gamma(\eta_0) \simeq 5 \times 10^{-6}, \qquad (18)$$

where $\Omega_\gamma(\eta_0) = 2.6 \times 10^{-5} \, h_0^{-2}$ is the fraction of critical energy density stored in radiation at the present observation time η_0; $f_{\text{ns}} \sim 10^{-10}$ Hz and f_{max} are, respectively, the nucleosynthesis frequency and the maximal frequency of the graviton spectrum (for our present example $f_{\text{max}} = f_1$). It is intuitively clear that if the spectrum is flat the BBN bound will be easily satisfied provided the theoretical amplitude of the spectrum, $\overline{\Omega}^{\text{th}}$ is roughly less than 10^{-6}. In the case of growing spectra the situation is more tricky. Let us denote with

$$h_0^2 \overline{\Omega}^{\text{max}} \simeq \frac{5 \times 10^{-6}}{\mathcal{I}} , \qquad \mathcal{I} = \int_{f_{\text{ns}}}^{f_{\text{max}}} \omega(f) \, \text{d} \ln f, \qquad (19)$$

the maximal normalization of the spectrum compatible with the BBN bound. The sensitivity to a given $\omega(f)$ (which now increases with f) will be always given by Eq. (11). We should however exclude from the parameter space of our theoretical model those regions where $\overline{\Omega} > \overline{\Omega}^{\text{max}}$. Thus, the regions of the parameter space of a given model for which $\overline{\Omega}^{\text{max}} > \overline{\Omega}$ are, simultaneously, visible by the VIRGO pair and compatible with the BBN. In the absence of a specific theoretical normalization this would be the end of the story. However, in some models one can also estimate (with a given accuracy) the theoretical normalization of the spectrum. For instance, in the case of string cosmological models, the theoretical normalization of the spectrum can be expressed as

$$\overline{\Omega}^{\text{th}} \simeq 2.6 \, g_1^2 \left(\frac{10^3}{n_r} \right)^{1/3} \Omega_\gamma(\eta_0) . \qquad (20)$$

The accuracy of this determination coincides with the accuracy in the determination of g_1 (the dilaton coupling at the beginning of the string phase) and of n_r as defined in Eq. (17).

9

If we want to compare the achievable sensitivity not only with the BBN bound but also with the theoretical normalization we will have to require that $\overline{\Omega}^{\mathrm{max}} > \overline{\Omega}$ and $\overline{\Omega}^{\mathrm{th}} > \overline{\Omega}$ are simultaneously satisfied. With these necessary specifications let us now analyze the impact of the maximization of the overlap in the case of non-scale-invariant spectra of string cosmological type. Our results for the ratios $\overline{\Omega}^{\mathrm{max}}/\overline{\Omega}$ and $\overline{\Omega}^{\mathrm{th}}/\overline{\Omega}$ are reported in Figs. 3, 4, and 5. In Fig. 3 we illustrate the sensitivity to string cosmological spectra under the assumption of maximal overlap (profile A of Fig. 2). The region in the left plot of Fig. 3 traces the area of the parameter space where $\overline{\Omega}^{\mathrm{max}} > \overline{\Omega}$, whereas the right plot corresponds to the region of the parameter space for which $\overline{\Omega}^{\mathrm{th}} > \overline{\Omega}$. The plots of Fig. 3 can be compared
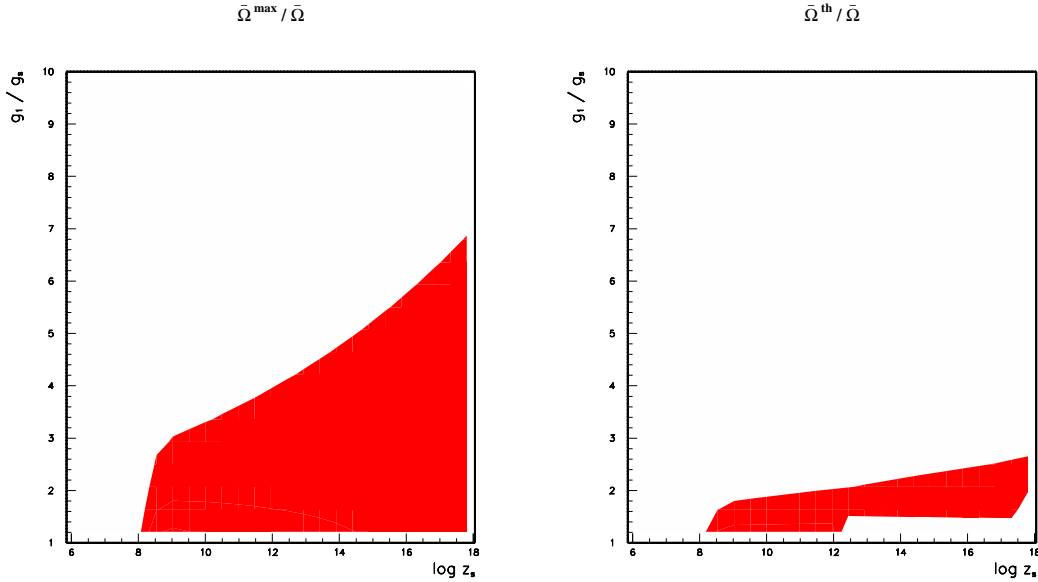

Figure 3: We illustrate the regions of the parameter space of non-scale-invariant spectra of string cosmological type. As a function of g_1/g_s and z_s we report the regions for which $\overline{\Omega}^{\mathrm{max}}/\overline{\Omega} > 1$ (left) and $\overline{\Omega}^{\mathrm{th}}/\overline{\Omega} > 1$. The overlap is assumed to be maximal (profile A of Fig. 2). The fiducial set of parameters chosen for these plots (and determining the maximal frequency of the spectrum) is $g_1 = 1/20$ and $n_r = 10^3$.

with the case where the overlap is not maximal. This is done in Figs. 4 and 5. In Fig. 4 the meaning of the shaded regions is exactly the same as in Fig. 3 but with the assumption of minimal overlap. In fact, the relevant profile of $\gamma(f)$ is the one labeled with C in Fig. 2. By comparing Fig. 3 with Fig. 4 we can notice that the effects of the maximization of the overlap is to increase the visibility region both in terms of $\overline{\Omega}^{\mathrm{max}}/\overline{\Omega}$ and in terms of $\overline{\Omega}^{\mathrm{th}}/\overline{\Omega}$. As far as the maximal values of these two ratios are concerned the effect of the overlap reduction is irrelevant. Thence, we can conclude that a maximization (minimization) of the overlap between the VIRGO detectors is more evident if the detectable spectrum is
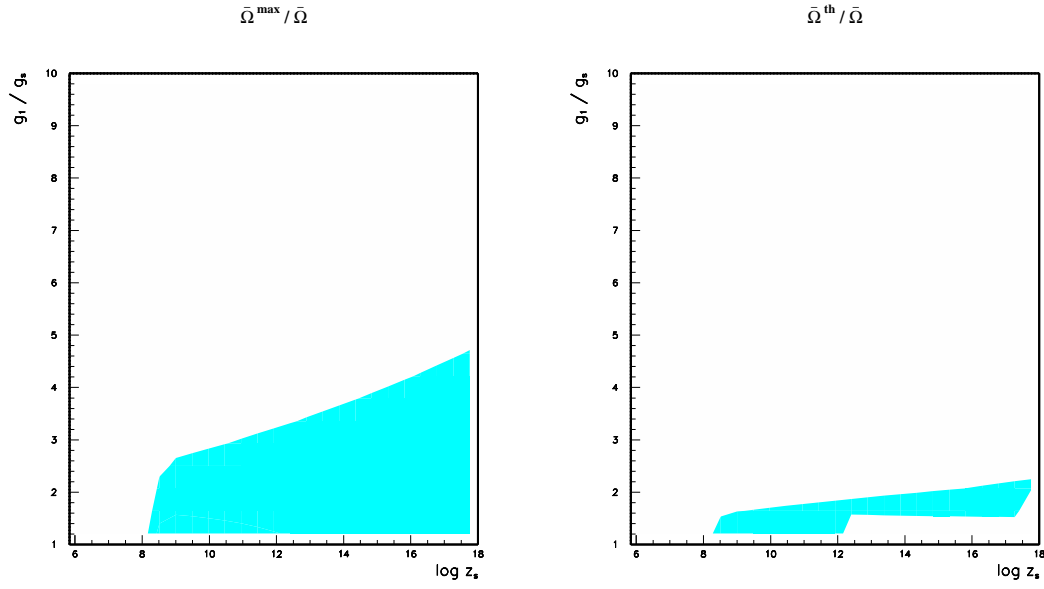
Figure 4: In order to make easier the comparison we report the same quantities discussed in Fig. 3, with the same fiducial choice of g_1 and n_r but under the assumption of minimal overlap, i.e. profile C in Fig. 2.
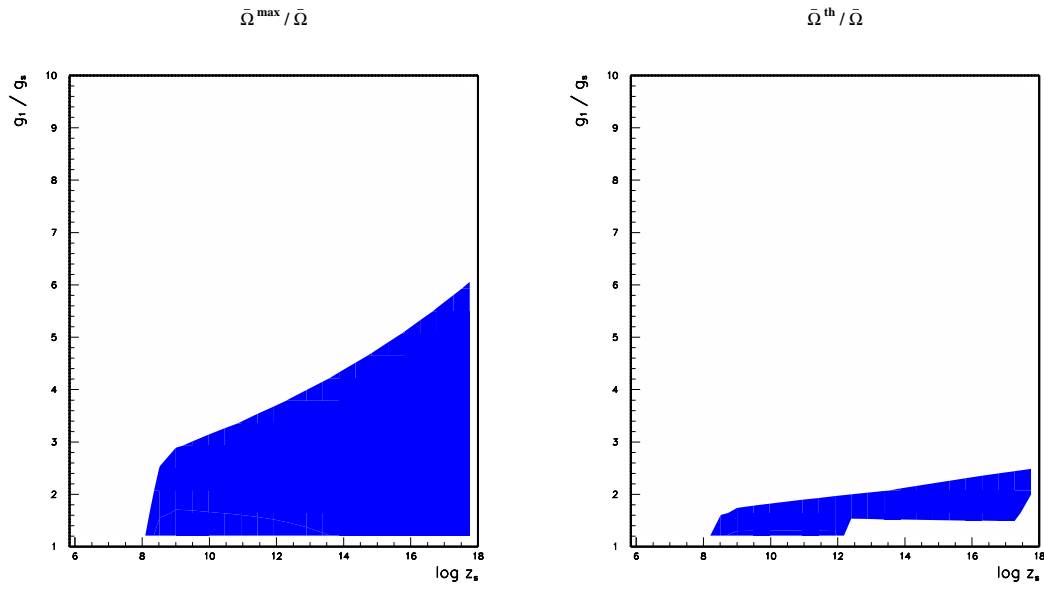

Figure 5: We report the same visibility region discussed in Fig. 3 and 4 but in the case of intermediate overlap, i.e. profile B in Fig. 2.

11

non-scale-invariant. In the latter case, an increase in the overlap can sizably enlarge our sensitivity to the parameter space of a given model.

For sake of completeness we also report in Fig. 5 the patterns of the visibility region for non-scale-invariant spectra in the case of intermediate overlap. In this case the two VIRGO detectors are assumed to be roughly 500 km apart and this corresponds to the profile B of Fig. 2. As we can see from Fig. 5 the area of the visibility region is, approximately, in between the ones obtained in the case of Figs. 3 and 4.

In order to complete our analysis we would like to discuss the simultaneous effect of overlap maximization and noise reduction since this is one of the open possibilities of the upgraded VIRGO program. Suppose, for instance, that the noise configuration of the upgraded VIRGO would correspond to a reduction vector $\vec{\rho} = (0.1, 0.01, 1)$. If the overlap is either maximal or minimal the visibility region are the ones reported in Fig. 6. In particular, in Fig. 6 we report the regions for which $\overline{\Omega}^{\rm th} > \overline{\Omega}$ (needless to say that we report only those
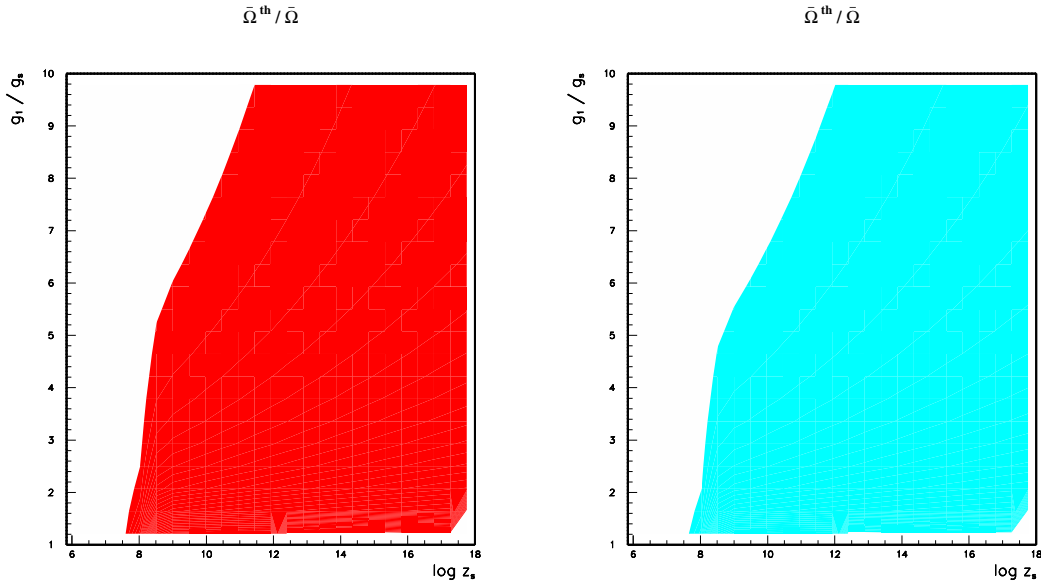

Figure 6: Under the assumption of selective thermal noise reduction we illustrate the behaviour of visibility region of the VIRGO pair in the case on growing logarithmic energy spectra of string cosmological type. We assumed a noise reduction vector $\vec{\rho} = (0.1, 0.01, 1)$. At the left the overlap is maximal whereas at the right the overlap is minimal. As in the previous plots we consider a fiducial set of parameters ($g_1 = 1/20$ and $n_r = 10^3$) to fix the maximal frequency. The sharp drop in the sensitivity after $z_s = 10^8$ can be understood by noticing that, in this case, $f_s \sim f_0 \sim 100$ Hz. As we can see by comparing the left plot to the right one, if the thermal noises are consistently reduced, the gain in overlap gets less relevant. This is not the case if the noise are not reduced.

12

regions of parameter space for which the BBN bound is satisfied, i.e. $\overline{\Omega}^{\text{th}} < \overline{\Omega}^{\text{max}}$). In the left plot of Fig. 6 we assumed maximal overlap (profile A of Fig. 2) whereas in the right plot we assumed minimal overlap (profile C of Fig. 2). As we can see, a joined reduction of thermal noises overwhelms almost completely the effect of the maximization of the overlap in the sense that, if the thermal noises are consistently reduced, the visibility region seems to be rather insensitive to the relative location of the two detectors. Similar conclusions (and similar plots) are obtained in the case of different reduction vectors affecting the thermal noises. Finally, if the shot noise contribution is reduced the sensitivity is only mildly affected [15]. The reason for this statement stems from the fact that the shot noise reduction starts being important for frequencies larger than the kHz (see Fig. 1) [15]. But for $f > 1$ kHz the overlap reduction is very efficient in spite of the location of the two detectors as it can be argued from Fig. 2.

6   Conclusion

The effect of maximization (or reduction) of the overlap of two coaligned VIRGO detectors depends upon the specific form of the logarithmic energy spectrum of relic gravitational waves backgrounds. If the spectra are purely scale-invariant the effect of minimization of the overlap are negligible. If the spectra are non-scale-invariant the maximization of the overlap has a sizable impact on the sensitivity.

If we simultaneously maximize the overlap and reduce (selectively) the contributions of the pendulum and pendulum's internal modes to the noise power spectra, the sensitivity of the VIRGO pair to a scale-invariant spectrum can be as low as 10^{-9} after one year of observations and with SNR = 1.

In the assumption that no noise reduction will take place in the context of the upgraded VIRGO program, the maximization of the overlap alone enlarges sizably the visibility window (always for $T = 1$ yr and SNR = 1) for the case of non-scale-invariant (and growing with frequency) logarithmic energy spectra. In the assumption of a consistent reduction of the thermal noises the sensitivity to growing logarithmic energy spectra increase significantly in spite of the location of the second VIRGO interferometer since, in the latter case, the good effect of the overlap maximization is overcome by the thermal noise reduction.

From a theoretical perspective, our results support the conclusion that the maximization of the overlap has a different impact depending upon the analytical form of the logarithmic energy spectrum, urging, in particular dedicated studies of the forthcoming data for the specific case of growing logarithmic energy spectra. From a purely experimental perspective our findings suggest that a simultaneous maximization of the overlap and a noise reduction in the pendulum and pendulum's internal modes is desirable and extremely useful for a decisive improvement in the sensitivity of the VIRGO pair.

Acknowledgments

We want to thank A. Giazotto for very interesting remarks and conversations.

References

[1] L. P. Grishchuk, Pis'ma Zh. Éksp. Teor. Fiz. **23**, 326 (1976) (JETP. Lett. **23**, 293 (1976)); K. S. Thorne, in *300 Years of Gravitation*, edited by S. W. Hawking and W. Israel (Cambridge University Press, Cambridge, 1987); L. P. Grishchuk, Usp. Fiz. Nauk. **156**, 297 (1988) (Sov. Phys. Usp. **31**, 940 (1988)).

[2] M. Giovannini M, Phys. Rev. D **58**, 083504 (1998).

[3] V. Kaspi, J. Taylor, and M. Ryba, Astrophys. J. **428**, 713 (1994).

[4] V. F. Schwartzman, Pis'ma Zh. Éksp. Teor. Fiz. **9**, 315 (1969) (JETP. Lett. **9**, 184 (1969)); T. Walker et al., Astrophys. J. **376**, 51 (1991); C. Copi et al., Phys. Rev. Lett. **75**, 3981 (1995); R. E. Lopez and M. S. Turner, Phys. Rev. D **59**, 103502 (1999).

[5] M. Giovannini, Class. Quantum Grav. **16** 2905 (1999); Phys. Rev. D **60** 123511 (1999); P. J. Peebles and A. Vilenkin, Phys. Rev. D **59** 063505 (1999).

[6] M. Gasperini and M. Giovannini, Class. Quantum Grav. **9**, L137 (1992); M. Giovannini, Phys. Rev. D **55**, 595 (1997).

[7] L. P. Grishchuk, talk given at 34th Rencontres de Moriond: *Gravitational Waves and Experimental Gravity*, Les Arcs, France, 23-30 Jan 1999, gr-qc/9903079; M. Giovannini, Phys. Rev. D **59**, 121301 (1999).

[8] G. Veneziano, Phys. Lett. B **265**, 287 (1991).

[9] M. Gasperini and M. Giovannini, Phys. Lett. B **282**, 36 (1992); Phys. Rev. D **47**, 1519 (1993); M. Gasperini, M. Giovannini, and G. Veneziano, Phys. Rev. D **48**, 439 (1993).

[10] B. Caron et al, Class. Quantum Grav. **14**, 1461 (1997).

[11] The importance of building an advanced european interferometers has been clearly stated in the *European Gravitational Wave Meeting*, London, 27 May 1999 (Giazotto A, private communication).

[12] P. Michelson, MNRAS **227**, 933 (1987); N. Christensen, Phys. Rev. D **46**, 5250 (1992).

[13] E. Flanagan, Phys. Rev. D **48**, 2389 (1993); B. Allen and J. D. Romano, Phys. Rev. D **59**, 102001 (1999).

[14] D. Babusci and M. Giovannini, Phys. Rev. D **60**, 083511 (1999).

[15] D. Babusci and M. Giovannini, gr-qc/9912035.

[16] E. Cuoco, G. Curci, and M. Beccaria, to appear in the *Proceedings of the 2nd Edoardo Amaldi Conference*, Geneva, Switzerland, gr-qc/9709041.

[17] P. R. Saulson, *Fundamentals of interferometric gravitational wave detectors* (World Scientific, Singapore, 1994).

[18] K. Danzmann, in *Gravitational Wave Experiments*, edited by E. Coccia, G. Pizzella, and F. Ronga (World Scientific, Singapore, 1995).

[19] V. Kaplunovsky, Phys. Rev. Lett. **55**, 1036 (1985).